International Journal of Advanced and Applied Sciences, 3(8) 2016, Pages: 43-51

Contents lists available at Science-Gate

International Journal of Advanced and Applied Sciences

Journal homepage: http://www.science-gate.com/IJAAS.html

Tracking control of an unmanned aerial vehicle using cascade configuration of fuzzy logic controllers in presence of windflaw

Mehdi Zare [1,*], Ehsan Zakeri [2], Jafar Sadeghi [3], Said Farahat [1]

[1]*Department of Mechanical Engineering, University of Sistan and Baluchestan, Zahedan, Iran*
[2]*Young Researchers and Elite Club, Shiraz Branch, Islamic Azad University, Shiraz, Iran*
[3]*Department of Chemical Engineering, University of Sistan and Baluchestan, Zahedan, Iran*

ARTICLE INFO

Article history:
Received 9 June 2016
Received in revised form
3 August 2016
Accepted 16 August 2016

Keywords:
Fuzzy logic controller
Octagonal helix path
Quadrotor
UAV
Under-actuated system

ABSTRACT

In this study, an unmanned aerial vehicle (UAV), quadrotor particularly, with six degree of freedom (6-DOF) is modeled and a novel arrangement of fuzzy logic controller (FLC) are designed to control quadrotor's attitude and altitude. The UAVs are high nonlinear in terms of dynamic equations and are in class of under-actuated systems with six degree of freedom and four propeller's speed as inputs. So, designing an appropriate controller is the main challenge in UAV's applications. The controller architectures is composed of three FLCs. A MIMO FLC is implemented to control angles and altitude which is fed by two first output controllers, namely desired roll and pitch angles. Then, an octagonal helix path is constructed in such a way that an octagonal schema is generated in X-Y plane and is developed in vertical direction. By applying the windflaw to the system as a disturbance, which is blew in three directions, namely x, y, and z, the performance of designed controller is investigated. Finally, results are presented to show the controller performance for tracking purpose in presence of a wind as disturbance.

© 2016 The Authors. Published by IASE. This is an open access article under the CC BY-NC-ND license (http://creativecommons.org/licenses/by-nc-nd/4.0/).

1. Introduction

In the last few years, scientists and researchers are interested in under-actuated systems, systems with fewer independent control actuators than degree of freedom to be controlled. Quadrotor is an under-actuated system since it has 6-DOF (position (x, y, z) and angles (roll, pitch, and yaw)) and four control input (four propeller's speeds). So, it is difficult to design efficient controller for quadrotor (Mian et al., 2008). Each of the rotors on the quad-rotor helicopter produces both thrust and torque. Given that the front and rear motors both rotate counter-clockwise and the other two rotate clockwise, the net aerodynamic torque will be zero. Early designs of quadrotor were performed in the 1907's by Louis Charles Bréguet (1880 - 1955) and then were developed by Étienne Edmond Oehmichen (1884-1955) and George de Bothezat (1882 – 1940). With advances in technology, quadrotors were extended in smaller size. Two model-based control techniques are applied to quadrotor by bouabdallah et al. (2004); a classical approach PID assuming simplified dynamics and a newer technique LQ (linear quadratic), based on more complete model (Bouabdallah et al., 2004). Pounds et al. (2006) are developed X-4 flyer with an onboard embedded attitude controller to stabilize flight. Also, a linear SISO (single input-single output) controller was designed to regulate flyer attitude (Pounds et al., 2006). In 2008s, a nonlinear model of an under-actuated quadrotor aerial robot is derived, based on Newton-Euler formalism, and back-stepping based PID control strategy is implemented for the derived model by Mian and Daobo (2008). A robust control methodology for a quadrotor mechanism is developed by Sangyam et al. (2010). Also, a conventional proportional-integral-derivative (PID) controller and self-tuning PID based on fuzzy logic are compared and analyzed (Sangyam et al., 2010). A fuzzy control is designed and implemented to control a simulation model of the quadrotor with the desired values of the height, roll, pitch and yaw are considered as the inputs, is presented by santo, et al, (2010). A design of a controller based on the block control technique combined with the super twisting control algorithm for trajectory tracking of a quadrotor helicopter is presented by Luque-Vega et

* Corresponding Author.
Email Address: m.zaare7631@gmail.com (M. Zare)
http://dx.doi.org/10.21833/ijaas.2016.08.008
2313-626X/© 2016 The Authors. Published by IASE.
This is an open access article under the CC BY-NC-ND license (http://creativecommons.org/licenses/by-nc-nd/4.0/)

al. (2012). A nested loops control architecture in implemented by Nagaty et al. (2013). A nonlinear Backstepping controller is implemented for the inner stabilization loop and the reference trajectories for the inner loop controller to reach the desired waypoint is generated by the outer loop controller. Moreover, to ensure boundedness of the reference trajectories, a PD controller with a saturation function is used for the outer loop (Nagaty et al., 2013). In (Rabhi et al., 2011) an algorithm based on robust fuzzy logic controller to ensure stabilization of the quadrotor is proposed. Also, other control methods are performed to control the quadrotor parameters, For instance, Lyapunov theory (Bouabdallah et al., 2004; Dzul et al., 2004; Lozano et al., 2004; Salazar-Cruz et al., 2005), linear quadratic regulator (LQR) (Lozano et al., 2005), dynamic feedback (Mokhtari and Benallegue, 2004; Mistler et al., 2001), neural networks (Tarbouchi et al., 2004), reinforcement learning (Waslander et al., 2005), and visual feedback (Guenard et al., 2008; Hamel et al., 2005).

In the following sections, the basic conceptions of the quadrotor movement are described since the FLC rules are depended to these maneuver descriptions. Then, in modelling section, the dynamic model of the quadrotor with 6-DOF is derived through robotic methods to implement the quadrotor system in MATLAB Simulink. Then, a novel arrangement of FLC is designed to control attitude and altitude of the quadrotor. An octagonal helix path is constructed in such a way that an octagonal schema is generated in X-Y plane and is developed in vertical direction constructed to validate the controller performance. Finally, simulation results are presented in result section.

2. Basic concept

The main advantages of the quadrotors are high maneuverability and vertical takeoff and landing (Alexis et al., 2011). All maneuvers are supplied through four basic maneuvers as shown in Fig. 1. These maneuvers and resultant movement are used to design FLC so that the quadrotor is stabled in the air (section 3).

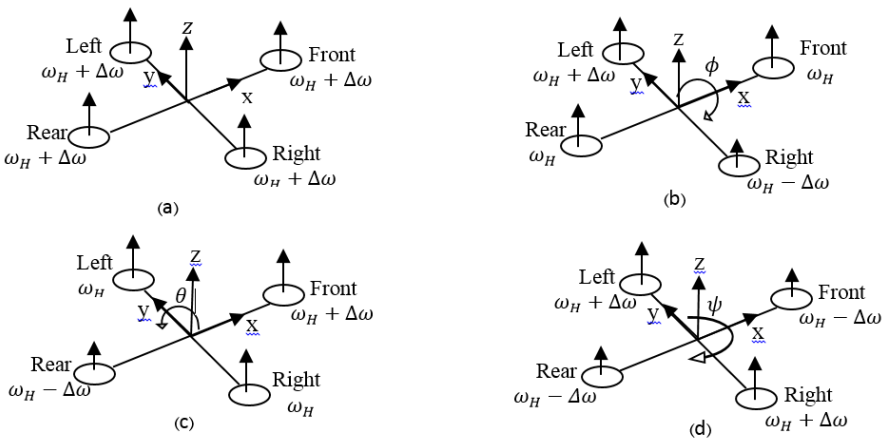

Fig. 1: Basic maneuvers of the quadrotor (Zare et al., 2104)

- Throttle movement: This movement is provided by increasing (decreasing) four propeller speeds simultaneously by the same amount (Fig. 1a). The quadrotor is raised, when the resultant forces of the propeller speeds are more than the gravity, and is moved down, when the resultant forces of the propeller speeds are less than the gravity. Also, the amount of Δω is enough small while the model of quadrotor eventually be influenced by strong nonlinearities.
- Roll maneuver: This maneuver is provided by increasing (decreasing) the left propeller speed and decreasing (increasing) the right one (Fig. 1b). It leads to a torque with respect to the x-axis which makes the quadrotor turn. Also, the overall vertical trust remains constant.
- Pitch maneuver: This maneuver is provided by increasing (decreasing) the front propeller speed and decreasing (increasing) the rear one (Fig. 1c). It leads to a torque with respect to the y-axis which makes the quadrotor turn. Also, the overall vertical trust remains constant.
- Yaw maneuver: This maneuver is provided by increasing (decreasing) the right and left propeller speeds and decreasing (increasing) the front and rear ones (Fig. 1d). It leads to a torque with respect to the y-axis which makes the quadrotor turn. Also, the overall vertical trust remains constant.

3. Mathematical model

In this section, mathematical model of the quadrotor with 6-DOF is derived through robotic and Newton-Euler method. Some assumption is considered to derive dynamic equations of the model. Two frames have to be defined:

- The earth inertia frame (E-frame),
- The body-fixed frame (B-frame).

The equations of motion are more conveniently formulated in the body-fixed frame because of the following reasons (Bresciani, 2008):

• The inertia matrix is time-invariant.
• Advantage of body symmetry can be taken to simplify the equations.
• Measurements taken on-board are easily converted to body-fixed frame.
• Control forces are almost always given in body-fixed frame.

A generic 6-DOF rigid body is defined as (Eq. 1):

$$\dot{\xi} = J_\theta v \tag{1}$$

where $\dot{\xi}$ is the generalized velocity vector with respect to E-frame, v is the generalized velocity vector with respect of B-frame and J_θ is the generalized matrix (Fig. 2).

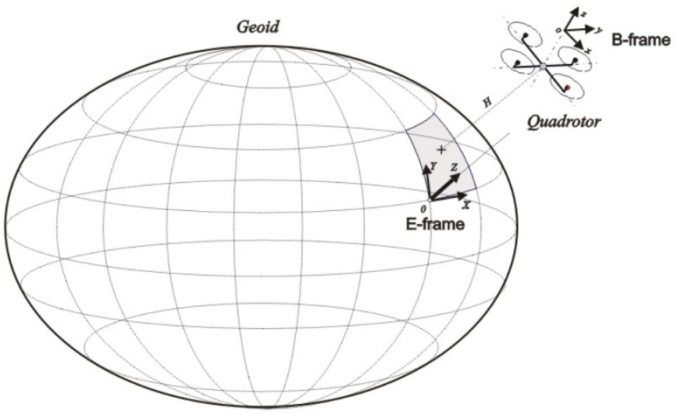

Fig. 2: The inertia Frame (E) and the body frame (B) (Rodić and Mester, 2011)

$\dot{\xi}$ is composed of the quadrotor linear Γ^E (m) and angular Θ^E (rad) position vector with respect to E-frame as (Eq. 2):

$$\xi = [\Gamma^E \theta^E]^T = [X\ Y\ Z\ \varphi\ \theta\ \psi]^T \tag{2}$$

Similarly, υ is composed of the quadrotor linear V^B $(\frac{m}{s})$ and angular ω^B $(\frac{rad}{s})$ position vector with respect to B-frame as (Eq. 3):

$$J_\theta = \begin{bmatrix} R_\Theta & 0_{3\times3} \\ 0_{3\times3} & T_\Theta \end{bmatrix} \tag{3}$$

The rotation R_Θ and the transfer T_Θ matrices are defined as (Eqs. 4 and 5):

$$R_\Theta = \begin{bmatrix} c_\psi c_\theta & -s_\psi c_\varphi + c_\psi s_\theta s_\varphi s_\psi s_\varphi + c_\psi s_\theta c_\varphi \\ s_\psi c_\theta c_\psi c_\varphi + s_\psi s_\theta s_\varphi & -c_\psi s_\varphi + s_\psi s_\theta c_\varphi \\ & -s_\theta c_\theta s_\varphi c_\theta c_\varphi \end{bmatrix} \tag{4}$$

$$T_\Theta = \begin{bmatrix} 1 & s_\varphi t_\theta c_\varphi t_\theta \\ 0 & c_\varphi \quad -s_\varphi \\ 0 & s_\varphi / c_\theta c_\varphi / c_\theta \end{bmatrix} \tag{5}$$

where $C_k = \cos k, S_k = \sin k, t_k = \tan k$.

The dynamic of a generic 6-DOF rigid body is obtained by Eq. 6:

$$\begin{bmatrix} mI_{3\times3} & 0_{3\times3} \\ 0_{3\times3} & I \end{bmatrix} \begin{bmatrix} \dot{V}^B \\ \dot{w}^B \end{bmatrix} + \begin{bmatrix} w^B \times (mV^B) \\ w^B \times (Iw^B) \end{bmatrix} = \begin{bmatrix} F^B \\ \tau^B \end{bmatrix} \tag{6}$$

where the notation $I_{3\times3}$ means a 3 times 3 identity matrix. $\dot{V}^B$ $(\frac{m}{s^2})$ is the quadrotor linear acceleration vector, $\dot{\omega}^b$ $\left(\frac{rad}{s^2}\right)$ is the quadrotor angular acceleration vector, F^B (N) is the quadrotor forces vector and τ^B (N.m) is the quadrotor torques with respect to B-frame. Also, two assumptions are considered in this approach. The first one states that the origin of the body fixed frame, O_B, is coincident with the center of mass (COM) of the body. Otherwise, another point (COM) should have been taken into account and it would have considerably complicated the body equations. The second one specifies that the axes of the B-frame coincide with the body principal axes of inertia. In this case the inertia matrix I is diagonal and, once again, the body equations become easier.

A generalized force vector Λ can be defined as (Eq. 7):

$$\Lambda = [F^B \tau^B] = \left[F_x F_y F_z \tau_x \tau_y \tau_z\right]^T \tag{7}$$

Therefore it is possible to rewrite Eq. 6 in matrix form, as (Eq. 8):

$$M_B \dot{\nu} + C_B(\nu)\, \nu = \Lambda \tag{8}$$

Where, M_B and C_B are system inertia and Coriolis-centripetal matrix, both with respect to B-frame, respectively.

The overall propeller's speed Ω $(\frac{rad}{s})$ and the propeller's speed vector $\mathbf{\Omega}$ $\left(\frac{rad}{s}\right)$ are defined as (Eq. 9):

$$\Omega = -\Omega_1 + \Omega_2 - \Omega_3 + \Omega_4 \qquad \mathbf{\Omega} = \begin{bmatrix} \Omega_1 \\ \Omega_2 \\ \Omega_3 \\ \Omega_4 \end{bmatrix} \tag{9}$$

where, Ω_1 $(\frac{rad}{s})$ is the front propeller speed, Ω_2 $(\frac{rad}{s})$ is the right propeller speed, Ω_3 $(\frac{rad}{s})$ is the rear propeller speed and Ω_4 $(\frac{rad}{s})$ is the left propeller speed.

The action of the movement vector on the quadrotor dynamics is shown as (Eq. 10):

$$U_B(\Omega) = E_B\Omega^2 = \begin{bmatrix} 0 \\ 0 \\ U_1 \\ U_2 \\ U_3 \\ U_4 \end{bmatrix} = \begin{bmatrix} 0 \\ 0 \\ b(\Omega_1^2+\Omega_2^2+\Omega_3^2+\Omega_4^2) \\ bl(\Omega_4^2-\Omega_2^2) \\ bl(\Omega_3^2-\Omega_1^2) \\ d(\Omega_2^2+\Omega_4^2-\Omega_1^2-\Omega_3^2) \end{bmatrix} \quad (10)$$

Where, l (m) is the distance between the center of the quadrotor and the center of propellers. U_1, U_2, U_3 and U_4 are the movement vector components introduced in the previous section. The movement matrix E_B is shown as (Eq. 11):

$$E_B = \begin{bmatrix} 0 & 0 & 0 & 0 \\ 0 & 0 & 0 & 0 \\ b & b & b & b \\ 0 & -bl & 0 & bl \\ -bl & 0 & bl & 0 \\ -d & d & -d & d \end{bmatrix} \quad (11)$$

It is possible to describe the quadrotor dynamics as (Eq. 12):

$$M_B\dot{\nu} + C_B(\nu)\nu = G_B(\xi) + O_B(\nu)\Omega + E_B\Omega^2 \quad (12)$$

By rearranging Eq. 12 it is possible to isolate the derivate of the generalized velocity vector with respect to B-frame $\dot{\nu}$ as (Eq. 13):

$$\dot{\nu} = M_B^{-1}\left(-C_B(\nu)\nu + G_B(\xi) + O_B(\nu)\Omega + E_B\Omega^2 + D_B\left(C_{x,y,z},\nu\right)\nu\right) \quad (13)$$

Where, G_B and $O_B$defined as (Eqs. 14 and 15):

$$G_B = \begin{bmatrix} F_G^B \\ 0_{3\times1} \end{bmatrix} = \begin{bmatrix} mgs_\theta \\ -mgc_\theta s_\varphi \\ -mgc_\theta c_\varphi \\ 0 \\ 0 \\ 0 \end{bmatrix} \quad (14)$$

$$O_B(\nu)\Omega = J_{TP}\begin{bmatrix} 0 & 0 & 0 & 0 \\ 0 & 0 & 0 & 0 \\ 0 & 0 & 0 & 0 \\ q & -q & q & -q \\ -p & p & -p & p \\ 0 & 0 & 0 & 0 \end{bmatrix}\Omega \quad (15)$$

Eq. 16 shows the previous expression not in a matrix form, but in a system of equations.
where, the propeller's speed input are given through the Eq. 17.

The Eq. 17 states the quadrotor dynamics in the body fixed frame. Eq. 18 shows Eq. 16 not in matrix form, but in system equations.

4. Fuzzy logic controller design

Fuzzy logic has been developed since 1965 by Zimmermann (2010). FLCs are used to control nonlinear systems special in a case of dynamic equations are complicated and only some information in system behavior is available. However, other model based controllers are depended on dynamic equations on the system. Moreover, the performance of the controller and stabilization of the system are independent of the uncertainties of the system, since fuzzy logic controller is designed regardless of the dynamic model and system parameters (Zakeri et al., 2016; Moezi et al., 2016; Moezi et al., 2014). Therefore, the controller is robust against uncertainties (Zakeri and Farahat, 2015).

$$\begin{cases} \dot{u} = (vr - wq) + g\,s_\theta \\ \dot{v} = (wp - ur) - g\,c_\theta s_\varphi \\ \dot{w} = (uq - vp) - g\,c_\theta c_\varphi + \frac{U_1}{m} \\ \dot{p} = \frac{I_{yy}-I_{zz}}{I_{xx}}qr - \frac{J_{TP}}{I_{xx}}q\Omega + \frac{U_2}{I_{xx}} \\ \dot{q} = \frac{I_{zz}-I_{xx}}{I_{yy}}pr + \frac{J_{TP}}{I_{yy}}P\Omega + \frac{U_3}{I_{yy}} \\ \dot{r} = \frac{I_{xx}-I_{yy}}{I_{zz}}pq + \frac{U_4}{I_{zz}} \end{cases} \quad (16)$$

$$\begin{cases} U_1 = b(\Omega_1^2+\Omega_2^2+\Omega_3^2+\Omega_4^2) \\ U_2 = bl(\Omega_4^2-\Omega_2^2) \\ U_3 = bl(\Omega_3^2-\Omega_1^2) \\ U_4 = d(-\Omega_1^2+\Omega_2^2-\Omega_3^2+\Omega_4^2) \\ \Omega = -\Omega_1+\Omega_2-\Omega_3+\Omega_4 \end{cases} \quad (17)$$

$$\begin{cases} \ddot{X} = \left(s_\psi s_\varphi + c_\psi s_\theta c_\varphi\right)\frac{U_1}{m} \\ \ddot{Y} = \left(-c_\psi s_\varphi + s_\psi s_\theta c_\varphi\right)\frac{U_1}{m} \\ \ddot{Z} = -g + \left(c_\theta c_\varphi\right)\frac{U_1}{m} \\ \dot{p} = \frac{I_{yy}-I_{zz}}{I_{xx}}qr - \frac{J_{TP}}{I_{xx}}q\Omega + \frac{U_2}{I_{xx}} \\ \dot{q} = \frac{I_{zz}-I_{xx}}{I_{yy}}pr + \frac{J_{TP}}{I_{yy}}P\Omega + \frac{U_3}{I_{yy}} \\ \dot{r} = \frac{I_{xx}-I_{yy}}{I_{zz}}pq + \frac{U_4}{I_{zz}} \end{cases} \quad (18)$$

In this study, a novel arrangement of FLCs is proposed to control the Quadrotor system. One MIMO FLC is designed to control roll, pitch, and yaw angles and altitude of the quadrotor. Two FLCs are also designed to feed third controller by suitable roll and pitch angles through controlling x and y position. So, there are two parallel FLCs which are connected to third FLC. The Takagi-Sugeno-Kang model is used to implementing FLC in following steps:

- Determining FLCs input: In all three controllers the error and error rate are considered as input in FLCs, which are determined by subtracting desired values from actual values. The error and error rate of x and y are considered as the controllers input

for the two first FLCs, respectively. The error and error rate of roll, pitch, and yaw angles and altitude of the quadrotor are considered as the third FLC input.

- Determining FLCs output: As mentioned, the third FLC is fed by the two first FLCs by appropriate roll and pitch angles. So, the outputs of two first FLCs are roll and pitch angles. The third FLC is connected to the system directly. As stated before, four propeller's speeds are considered as the system input, therefore, these angular speeds are considered as FLC outputs.
- Determining membership functions (MFs): In this system, there are five MFs for each input variable determining by very small to very big and considering as triangular and trapezoidal functions, as bellow (Eq. 19):

$$MF_{-2}, MF_{-1}, MF_0, MF_{+1}, MF_{+2} \quad (19)$$

Also, the general schema of the MFs is shown in the Fig. 3.

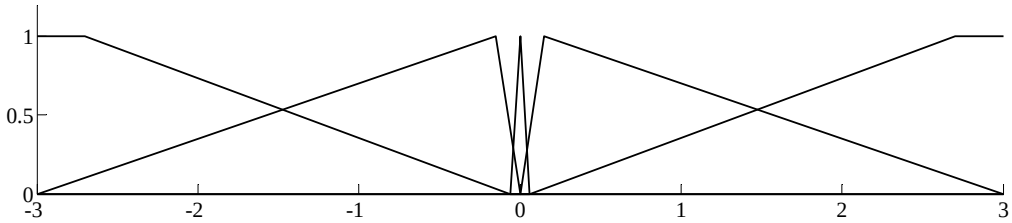

Fig. 3: The MFs schema

- Determining fuzzy rules: Fuzzy rules are designed based on behavior of the system through experience or human-liked sense. The network output is obtained by weighted average of fuzzy rules consequence output value since the TSK model gives the crisp numbers. There are nine consequences value by considering five MFs, as below (Eq. 20):

$$O_i = \{O_{-4}\ O_{-3}\ O_{-2}\ O_{-1}\ O_0\ O_{+1}\ O_{+2}\ O_{+3}\ O_{+4}\} \quad (20)$$

Fuzzy rules are obtained by evaluating relation of propeller's speeds and the UAV movements, as follows:

- Longitudinal movement: This movement achieved by increasing (decreasing) pitch angle. So, the fuzzy rules for longitudinal movement given by (Eq. 21):

if error is MF_i and error rate is MF_j then Ω_{Front} and Ω_{Rear} is constant, Ω_{left} is O_{i+j} and Ω_{right} is $O_{-(i+j)}$ (21)

- Transvers movement: This movement achieved by increasing (decreasing) pitch angle. So, the fuzzy rules for transvers movement given by (Eq. 22):

if error is MF_i and error rate is MF_j then Ω_{Right} and Ω_{Left} is constant, Ω_{Front} is O_{i+j} and Ω_{Rear} is $O_{-(i+j)}$ (22)

- Vertical movement: This movement achieved by increasing (decreasing) pitch angle. So, the fuzzy rules for vertical movement given by (Eq. 23):

if error is MF_i and error rate is MF_j then Ω_{Front}, Ω_{Rear}, Ω_{left}, and Ω_{right} is O_{i+j} (23)

- Rotational movement: This movement achieved by increasing (decreasing) the right and left propeller speeds and decreasing (increasing) the front and rear ones. So, the fuzzy rules for rotational movement given by (Eq. 24):

if error is MF_i and error rate is MF_j then Ω_{Front} is O_{i+j} and Ω_{Rear} is O_{i+j}, Ω_{left} is $O_{-(i+j)}$ and Ω_{right} is $O_{-(i+j)}$ (24)

Totally, the relation of MFs and fuzzy rules for two first controllers is shown in Table 1. Since the relation of MFs and fuzzy rules are hard to show in table form, the third FLC is presented earlier by formula.

Table 1: Relation of MFs and fuzzy rules

error rate / error	MF_{-2}	MF_{-1}	MF_0	MF_{+1}	MF_{+2}
MF_{-2}	O_{-4}	O_{-3}	O_{-2}	O_{-1}	O_0
MF_{-1}	O_{-3}	O_{-2}	O_{-1}	O_0	O_{+1}
MF_0	O_{-2}	O_{-1}	O_0	O_{+1}	O_{+2}
MF_{+1}	O_{-1}	O_0	O_{+1}	O_{+2}	O_{+3}
MF_{+2}	O_0	O_{+1}	O_{+2}	O_{+3}	O_{+4}

The FLCs configuration dealing with mentioned inputs and outputs and wind as a disturbance are shown in the Fig. 4.

5. Path planning

In this section, path generating procedure is presented and an octagonal helix path is developed. First, an octagonal schema is constructed in $x-y$ plane and then is extended in vertical direction, for making octagonal helix path, which is shown in Fig. 5.

6. Simulation results

In this section, the behavior of system in presence of wind as a disturbance is presented by applying a

novel configuration of FLCs. As mentioned, an octagonal helix path is considered as desired signal. Then, a wind disturbance is applied to the system input by sinusoidal function. The schematic of the system in presence of disturbance is shown in the Fig. 6. The sinusoidal wind applying to the system is determined as shown in Eqs. 25-27.

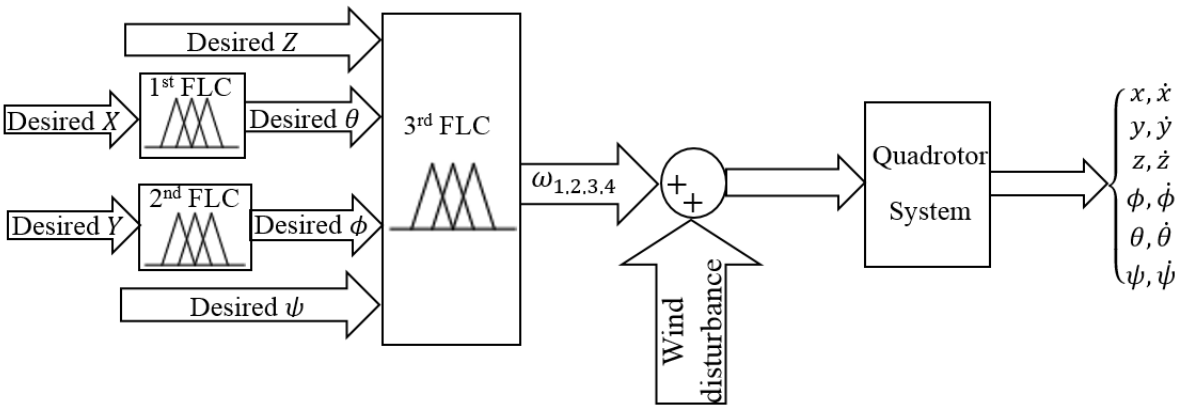

Fig. 4: System schematic with controllers in presence of wind as a disturbance

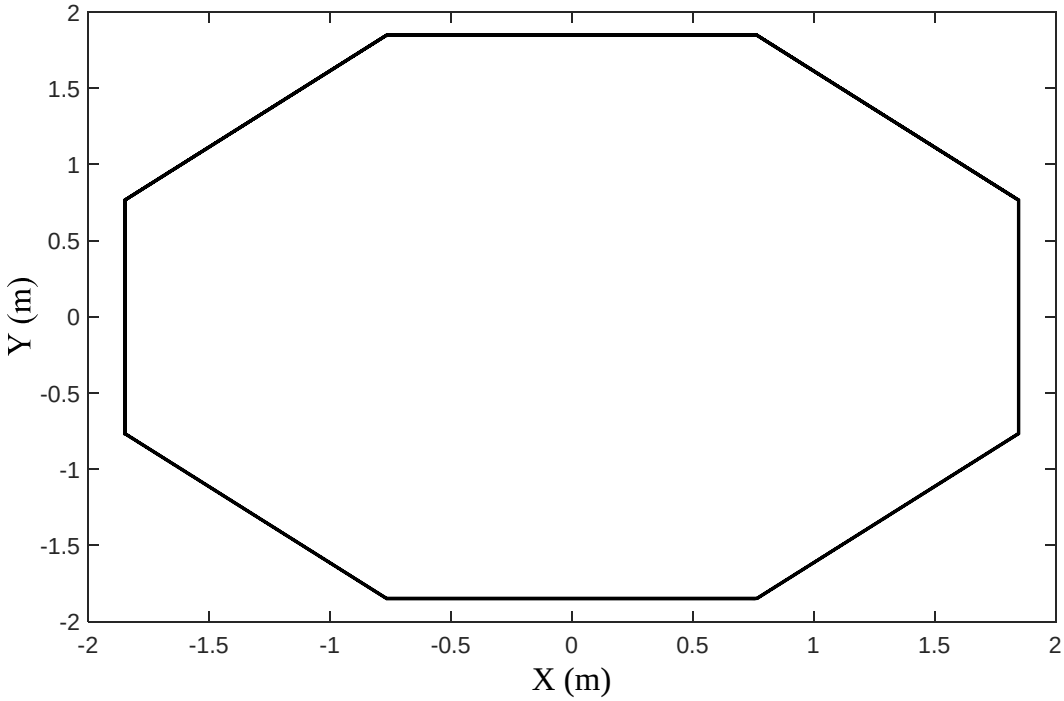

(a)

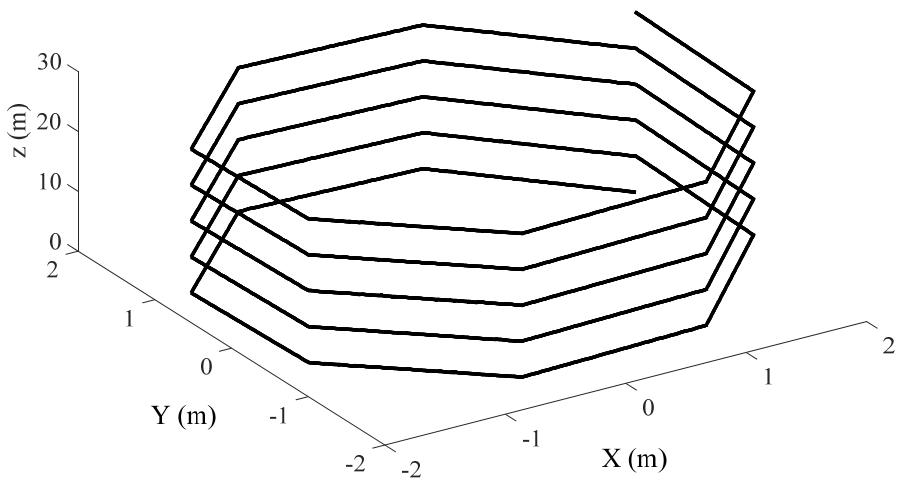

(b)

Fig. 5: a) Octagonal schema in the x − y plane, b) Octagonal helix path

$$D(x) = 0.5\sin(t) \quad (25) \qquad D(y) = 0.5\sin(t) \quad (26)$$

$$D(z) = 0.5\sin(t) \tag{27}$$

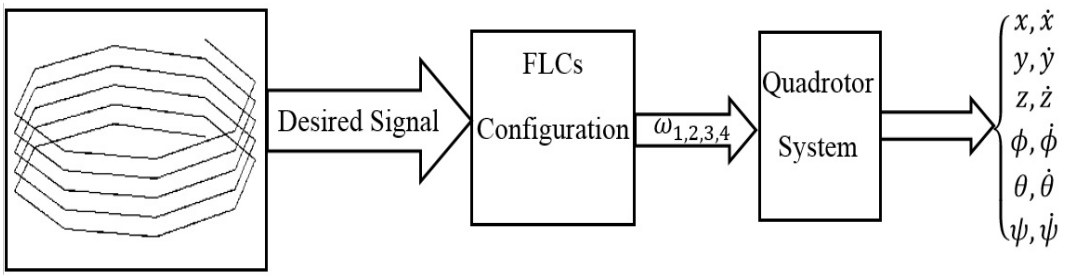

Fig. 6: The schematic of the system in presence of disturbance.

In the following Figs, behavior of the system is presented both in presences of disturbance and without disturbance. The results are shown in Figs. 7 to 10.

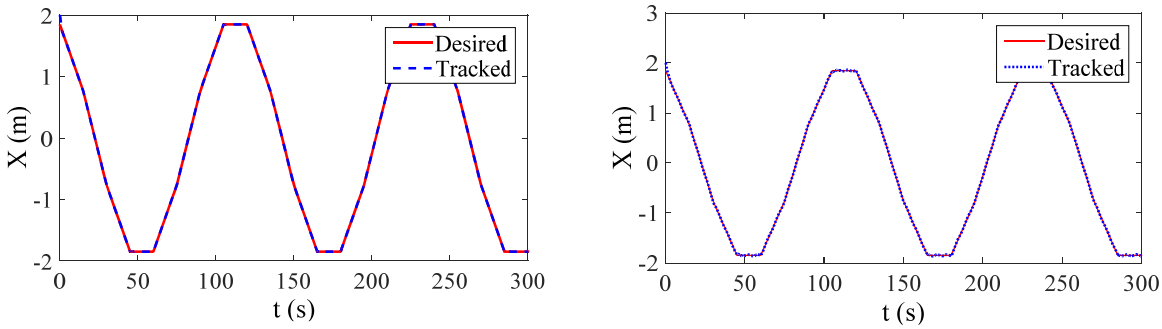

(a) Without disturbance (b) In presence of disturbance

Fig. 7: Path tracking in X direction

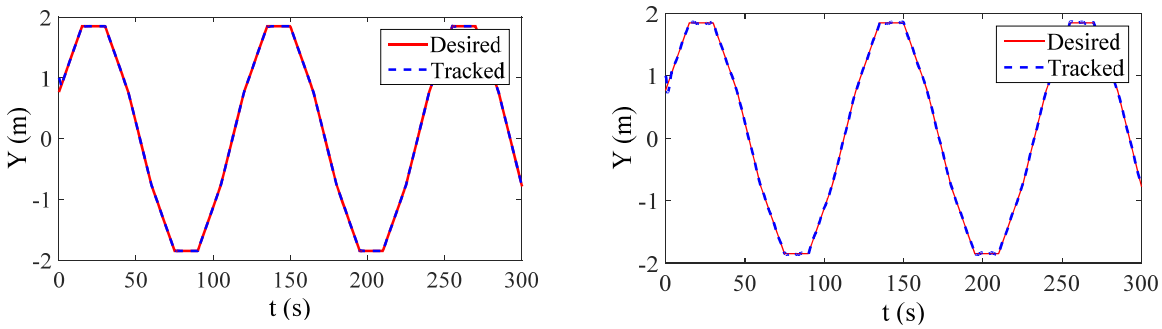

(a) Without disturbance (b) In presence of disturbance

Fig. 8: Path tracking in Y direction

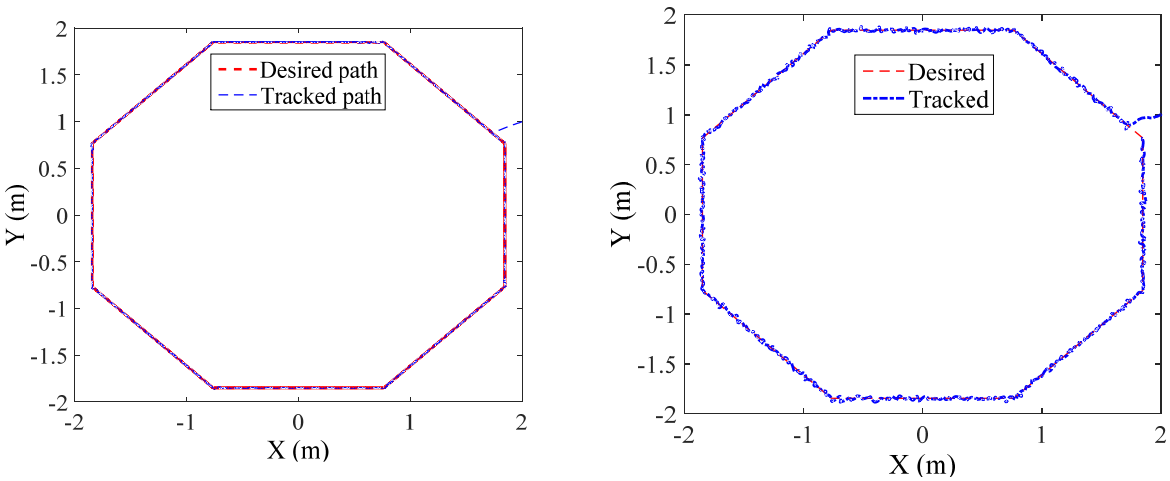

(a) Without disturbance (b) In presence of disturbance

Fig. 9: Octagonal Path tracking in X – Y plane

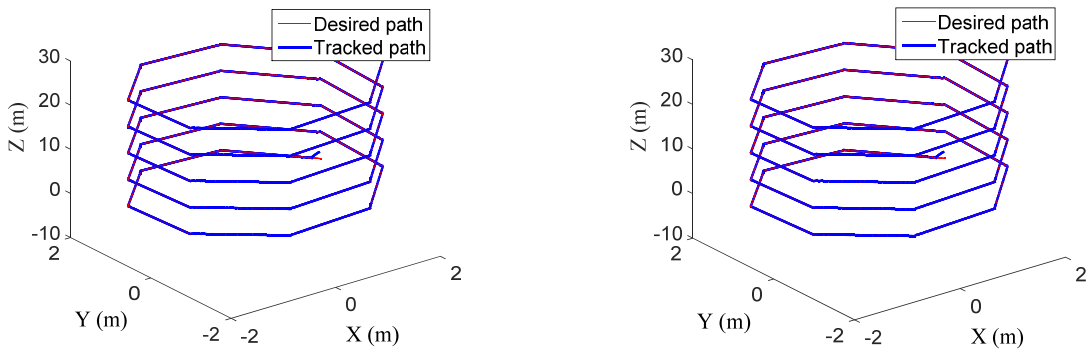

(a) Without disturbance (b) In presence of disturbance

Fig. 10: Octagonal helix path tracking

7. Conclusion

In this study, the dynamic mode of the quadrotor with 6-DOF is derived and simulated in MATLAB Simulink. The main contribution of this research is focuses on the development of the FLCs with a novel configuration to control the quadrotor system. An octagonal schema is constructed in the horizontal plane and is developed in vertical direction to create octagonal helix path as a desired. Then, a performance of the controller is evaluated by simulation result for tracking purpose in the desired path. Moreover, a wind in considered as a disturbance with sinusoidal function. According to the results, the proposed arrangement of the controllers are effective and the system is imitated the desired path in presence of the sinusoidal wind as a disturbance.

References

Alexis K, Nikolakopoulos G and Tzes A (2011). Switching model predictive attitude control for a quadrotor helicopter subject to atmospheric disturbances. Control Engineering Practice, 19(10): 1195-1207.

Bouabdallah S, Murrieri P and Siegwart R (2004). Design and control of an indoor micro quadrotor. In the IEEE International Conference on Robotics and Automation (ICRA'04), Barcelona, Spain, 5: 4393-4398

Bouabdallah S, Noth A and Siegwart R (2004, September). PID vs LQ control techniques applied to an indoor micro quadrotor. In the IEEE/RSJ International Conference Intelligent Robots and Systems (IROS 2004), Sendai, Japan, 3:2451-2456

Bresciani T (2008). Modelling, identification and control of a quadrotor helicopter. M.Sc. Thesis, Department of Automatic Control, Lund University.

Castillo P, Dzul A and Lozano R (2004). Real-time stabilization and tracking of a four-rotor mini rotorcraft. IEEE Transactions on Control Systems Technology, 12(4): 510-516.

Castillo P, Lozano R and Dzul A (2005). Stabilization of a mini rotorcraft with four rotors. IEEE Control Systems Magazine, 25(6): 45-55.

Dunfied J, Tarbouchi M and Labonte G (2004). Neural network based control of a four rotor helicopter. In the IEEE International Conference on Industrial Technology (ICIT'04), 3: 1543-1548

Guenard N, Hamel T and Mahony R (2008). A practical visual servo control for an unmanned aerial vehicle. IEEE Transactions on Robotics, 24(2): 331-340.

Lozano R, Castillo P and Dzul A (2004). Stabilization of a mini rotorcraft having four rotors. In the IEEE/RSJ International Conference on Intelligent Robots and Systems, Sendai, Japan: 2693-2698.

Luque-Vega L, Castillo-Toledo B and Loukianov AG (2012). Robust block second order sliding mode control for a quadrotor. Journal of the Franklin Institute, 349(2): 719-739.

Metni N, Hamel T and Derkx F (2005). Visual tracking control of aerial robotic systems with adaptive depth estimation. In the 44th IEEE Conference on Decision and Control, Seville, Spain: 6078-6084

Mian AA and Daobo W (2008). Modeling and backstepping-based nonlinear control strategy for a 6 DOF quadrotor helicopter. Chinese Journal of Aeronautics, 21(3): 261-268.

Mian AA, Ahmad MI and Wang D (2008). Backstepping based PID control strategy for an underactuated aerial robot. IFAC Proceedings Volumes, 41(2): 15636-15641.

Mistler V, Benallegue A and M'sirdi NK (2001). Exact linearization and noninteracting control of a 4 rotors helicopter via dynamic feedback. In the 10th IEEE International Workshop on Robot and Human Interactive Communication: 586-593

Moezi SA, Rafeeyan M, Zakeri E and Zare A (2016). Simulation and experimental control of a 3-RPR parallel robot using optimal fuzzy controller and fast on/off solenoid valves based on the PWM wave. ISA Transactions, 61: 265-286.

Moezi SA, Zakeri E, Bazargan-Lari Y and Khalghollah M (2014). Fuzzy logic control of a ball on sphere system. Advances in Fuzzy Systems, 17:1-6.

Mokhtari A and Benallegue A (2004). Dynamic feedback controller of Euler angles and wind parameters estimation for a quadrotor unmanned aerial vehicle. In the IEEE International Conferenc on Robotics and Automation (ICRA'04), Barcelona, Spain, 3: 2359-2366

Nagaty A, Saeedi S, Thibault C, Seto M and Li H (2013). Control and navigation framework for quadrotor helicopters. Journal of Intelligent and Robotic Systems, 70(1-4): 1-12.

Pounds P, Mahony R and Corke P (2006). Modelling and control of a quad-rotor robot. In the Australasian Conference on Robotics and Automation (ACRA 2006), Auckland, New Zealand.

Rabhi A, Chadli M and Pegard C (2011). Robust fuzzy control for stabilization of a quadrotor. In the IEEE 15th International Conference on Advanced Robotics (ICAR): 471-475

Rodić A and Mester G (2011). The modeling and simulation of an autonomous quad-rotor microcopter in a virtual outdoor scenario. Acta Polytechnica Hungarica, 8(4): 107-122.

Salazar-Cruz S, Palomino A and Lozano R (2005, December). Trajectory tracking for a four rotor mini-aircraft. In the 44th IEEE Conference on Decision and Control: 2505-2510.

Sangyam T, Laohapiengsak P, Chongcharoen W and Nilkhamhang I (2010). Path tracking of UAV using self-tuning PID controller based on fuzzy logic. In the SICE Annual Conference. IEEE: 1265-1269

Santos, M., Lopez, V., and Morata, F. (2010, November). Intelligent fuzzy controller of a quadrotor. In the IEEE International Conference on Intelligent Systems and Knowledge Engineering (ISKE): 141-146

Waslander SL, Hoffmann GM, Jang JS and Tomlin CJ (2005). Multi-agent quadrotor testbed control design: Integral sliding mode vs. reinforcement learning. In the IEEE/RSJ International Conference on Intelligent Robots and Systems: 3712-3717

Zakeri E and Farahat S (2015). Safe path planning and control of an Unmanned Underwater Vehicle (UUV) using particle swarm optimization and fuzzy logic control method. Moadres Mechanical Engineering, 14(14): 199-210.

Zakeri E, Farahat S, Moezi SA and Zare A (2016). Path Planning for Unmanned Underwater Vehicle in 3D Space with Obstacles Using Spline-Imperialist Competitive Algorithm and Optimal Interval Type-2 Fuzzy Logic Controller. Latin American Journal of Solids and Structures, 13(6): 1054-1085.

Zare M, Sadeghi J, Farahat S, and Zakeri E (2014). Regulating and helix path tracking for unmanned aerial vehicle (UAV) using fuzzy logic controllers. Journal of Mathematics and Computer Science, 13(1): 71-89.

Zimmermann HJ (2010). Fuzzy set theory. Wiley Interdisciplinary Reviews: Computational Statistics, 2(3): 317-332.